▸원 저◂ ISSN 1226-2854

Development of 14″×8.5″ active matrix flat-panel digital x-ray detector system and Imaging performance

— 평판 디지털 X-ray 검출기의 개발과 성능 평가에 관한 연구 —

Dept. of Biomedical Engineering Graduate School, Inje University
Medical Imaging Research Center of Inje University*

Ji-Koon Park · Jang-Yong Choi · Sang-Sik Kang
Dong-Gil Lee · Dae-Woo Seok · Sang Hee Nam*

— ABSTRACT —

Digital radiographic systems based on solid-state detectors, commonly referred to as flat-panel detectors, are gaining popularity in clinical practice. Large area, flat panel solid state detectors are being investigated for digital radiography. The purpose of this work was to evaluate the active matrix flat panel digital x-ray detectors in terms of their modulation transfer function (MTF), noise power spectrum (NPS), and detective quantum efficiency (DQE). In this paper, development and evaluation of a selenium-based flat-panel digital x-ray detector are described. The prototype detector has a pixel pitch of 139 ㎛ and a total active imaging area of 14×8.5 inch^2, giving a total 3.9 million pixels.

This detector include a x-ray imaging layer of amorphous selenium as a photoconductor which is evaporated in vacuum state on a TFT flat panel, to make signals in proportion to incident x-ray. The film thickness was about 500 ㎛. To evaluate the imaging performance of the digital radiography(DR) system developed in our group, sensitivity, linearity, the modulation transfer function(MTF), noise power spectrum (NPS) and detective quantum efficiency(DQE) of detector was measured. The measured sensitivity was 4.16×10^6 ehp/pixel · mR at the bias field of 10 V/㎛ : The beam condition was 41.9 KeV. Measured MTF at 2.5 lp/mm was 52%, and the DQE at 1.5 lp/mm was 75%. And the excellent linearity was showed where the coefficient of determination (r^2) is 0.9693.

Key words : Digital Radiography, thin film transistor, Modulation transfer function, Noise power spectrum, Detective quantum efficiency, selenium

Ⅰ. INTRODUCTION

Film/screen has been used to acquire the conventional radiographic examinations by capturing the pattern of x-rays transmitted through a patient. Recently, however, active matrix flat-panel imagers are beginning to replace the sheets of film[1-3]. These detectors use either the indirect or

the direct method to detect x-ray. Indirect detectors convert x-rays to visible light at the scintillating layer. And then this visible light is again converted to electric signal in photodiode. After that, the electrical signal is acquired by the readout component of the imaging system.

On the other hand, a direct detector directly converts x-rays to electric charges within a photoconductive layer[4-5]. Amorphous selenium (a-Se) usually has been used for this photoconductive material. The demand for DR systems is increasing because it is expected to solve some problems of analog radiographic systems such as the exhaustion of storage space, film management, and environmental pollution. A direct a-Se based flat panel x-ray detector has been developed for the first time in Korea.

The quantitative assessment of image quality of this x-ray detector is an important consideration in any type of imaging system. Several quantitative parameters have been devised that correlate with the abilities of imaging devices to perform clinical asks[6-8]. The concepts of modulation transfer function (MTF), noise power spectrum (NPS) and detective quantum efficiency (DQE) have been well described with sensitivity and linearity of detector and are very useful descriptors of resolution and signal-to-noise ratio. Such parameters were examined for evaluating a performance of this system.

II. PROTOTYPE DETECTOR SYSTEM DESCRIPTION

Our digital radiography system is constructed using a multi-layer structure consisting of an amorphous silicon thin-film transistor array, selenium as a photoconductor, and a dielectric layer. This device is normally operated at an electric field of 10V/㎛ to improve the transport of charge carrier.

Table 39. Specification of the prototype detector

	Specification	Unit
Array Format	2560×1536	pixels
Active area	14"×8.5"	Inch
Pixel Pitch	139	㎛
Film Thickness	500(a-Se)	㎛
Readout time	2.4	sec

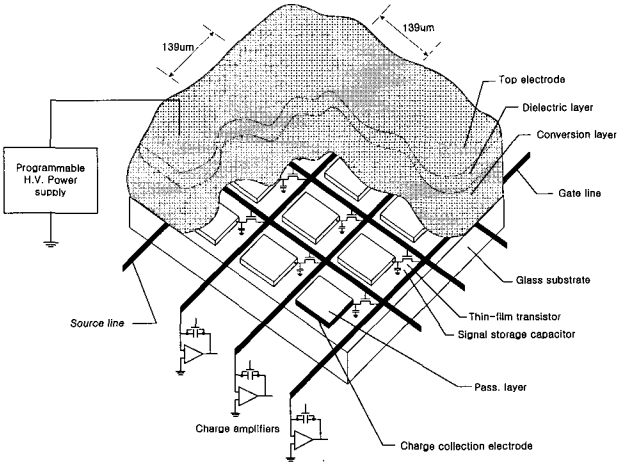

(a) Schematic cross-section

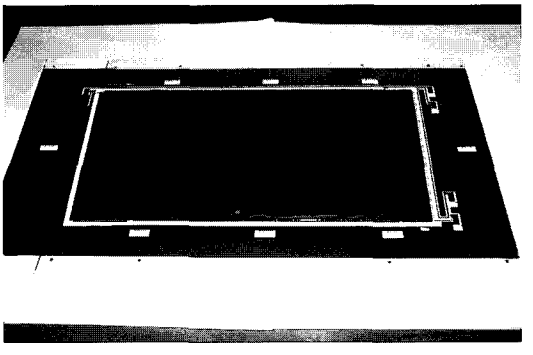

(b) 14"×8.5" Digital Radiography system

Fig. 1. Schematic flat-panel detector & photography of Digital radiography using a-Se

We investigate the basic imaging performance the prototype digital radiography detectors. The prototype digital x-ray detector consists of a 500㎛ thick amorphous selenium layer with $14\times8.5\,inch^2$ field of view. The main specification of the prototype detectors are summarized in Table 1.

Fig. 1 illustrates the schematic cross sections and photograph of the detector structure. The a-Se

film is directly deposited on a TFT array substrate, and a metal electrode, to which a bias voltage is applied, is then sequentially deposited by evaporation.

III. IMAGING PERFORMANCE

In this section we describe some experimental results including sensitivity, linearity, modulation transfer function, noise power spectrum, and detective quantum efficiency. For measuring sensitivity and linearity, the signal performance of the imaging system was quantitatively measured by the pixel signal size per unit exposure. Then MTF and NPS were measured by the method of Fujita et al. as adapted by Dobbins et al. Then DQE was calculated by a well-known equation[14].

1. Sensitivity

Sensitivity can be defined in terms of the charge produced by the detector per incident x-ray quanta of a specified energy. The sensitivity of imaging system depends on quantum efficiency and on primary conversion efficiency such as optical quanta or electric charge[9-11]. The sensitivity of the detectors was measured as a function of radiation exposure. We used the exposure range from 0.001 mR to 10 mR. The exposure levels were measured with ion chamber (2060 Radical. Corp.). Fig. 2 shows the schematic of sensitivity measurements system and the measured charge outputs per pixel · mR for the a-Se imaging detector. The results show the 4.16×10^6 ehp/pixel · mR at the bias field of 10 V/㎛ : The beam condition was 41.9 KeV.

2. Linearity

The linearity of the digital detector was determined for the relationship between input intensity and output signal in an imaging system. The response is referred to as the characteristic curve of the detector. In case of film/screen have a characteristic curve of sigmoid shape that is linear over about 1 to 2 orders of magnitude with respect to the logarithm of exposure intensity. For a precise experiment, we use a ion chamber of high quality exposure meter. The range of exposure value to be evaluated were made from 5 mR to 75 mR by changing mA. The low exposures were acquired using a low dose at 5 mR and heavy filtration (2 mm Al), whereas the high exposures were obtained at 75.5 mR and no added filtration. Measurements were made in a large enough ROIs (1 cm×1 cm) located over the detector. The mean pixel intensity value in these ROIs was averaged with standard deviation. Pixel value were corrected using "offset" correction factor. Data in Fig. 3 Show the response of the digital detector at the various exposure levels. This data demonstrate the excellent linearity response of the

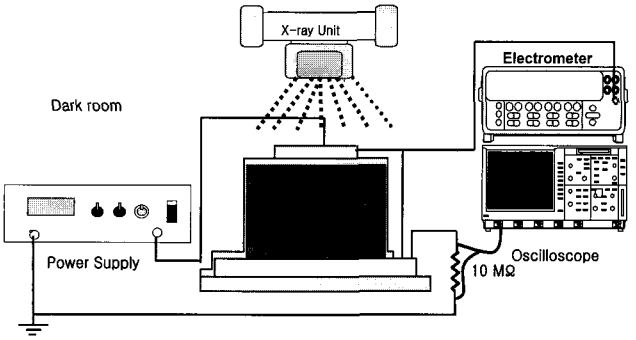

(a) schematic of sensitivity measurement system

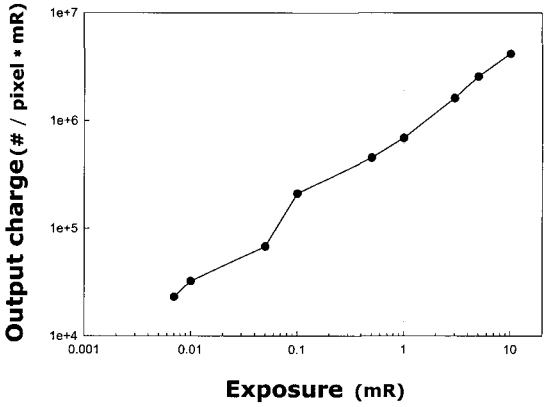

(b) Sensitivity of Digital radiography

Fig. 2. The schematic of sensitivity measurements system and the measured charge outputs per pixel · mR for the a-Se imaging detector

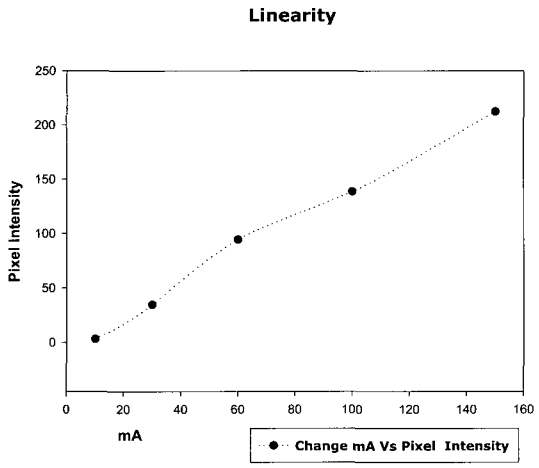

Fig. 3. the response of the digital detector at the various exposure levels

digital x-ray detector. The dotted line is a least squares fit to the experimental data points. And the coefficient of determination (r^2) is 0.9693.

3. Modulation Transfer Function

The MTF traditionally has been described mathematically in two ways by Dobbins III[15].

(1) as the ratio of frequency content output vs frequency content input

$$MTF(u,v) = \frac{|FT_{out}(u,v)|}{|FT_{in}(u,v)|} \quad \cdots\cdots (1)$$

(2) as the Fourier amplitude of the response to a delta function input to the system

$$MTF(u,v) = |OTF(u,v)| \quad \cdots\cdots (2)$$

where OTF(u,v) is the optical transfer function, the Fourier transform (FT) of PSF. Both of these descriptions are equivalent for systems without aliasing. For measuring MTF, we used the method of Fujita et al. as adapted by Dobbins et al[12,13]. The pre-sampling MTFs were determined using a tilted-slit method. A slightly tilted x-ray slit camera was imaged to measure the line spread functions(LSF). LSFs from subsequent lines were then combined into an effectively over-sampled LSF, which was then used to compute the pre-sampling MTF. The line spread function (LSF) was obtained by acquiring images of a narrow slit

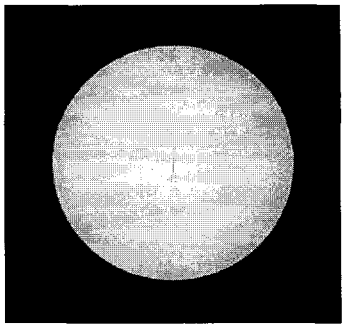

(a) The narrow slit with slightly slanted angle

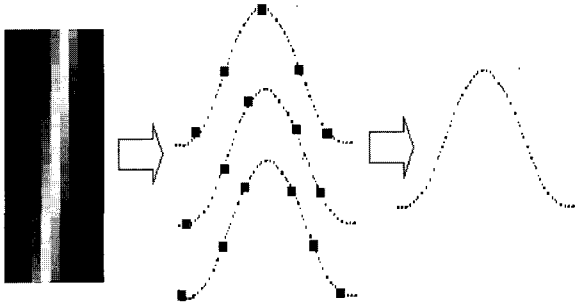

(b) Composite LSF

Fig. 4. Magnified micro-slit x-ray image and composite LSF obtained from several intensity profile

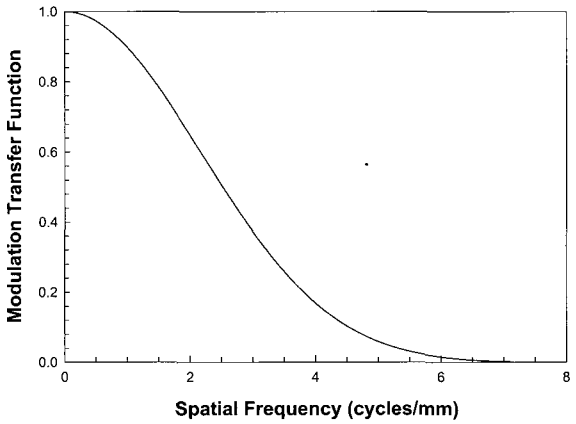

Fig. 5. Presampled MTF in DR system obtained by slit method

camera [Nuclear Associate model 07-624] which has very thin slit width of 10㎛ was used. For each measurement, the slit camera was placed right in front of the detectors to minimize image parallax and focal spot blurring. The slit was positioned at a slight angle(2~3°). This arrangement was used to generate a series of LSFs with the slit center positioned at various locations between two sam-

pling points. These LSFs were then combined into a single LSF with effectively many more sampling points or a much shorter sampling distance. It could eliminate an aliasing effect produced by discrete data sampling. The small focal spot (0.6 mm) was used to reduce focal spot blurring in MTF measurement. The Fourier Transform (FT) was then applied to the finely sampled LSF. X-ray image was obtained by aligning the narrow slit with slightly slanted angle to the pixel line of the DR detector system as shown in Fig. 4(a). Fig. 4(b) shows composite LSF obtained by combining several intensity profiles of slit in image.

Presampled MTF curve shown in Fig. 5 was obtained from finite composite LSF at 0~6 lp/mm using Fourier transform. Extrapolating operation was applied to 0.01% of maximum value of the LSF curve. Percent modulation values were 88% and 38% at the spatial frequencies of 1 lp/mm and 3 lp/mm, respectively.

4. Noise Power Spectrum

Noise power spectrum (NPS) could be thought of as the variance of image intensity divided among the various frequency components of the image. Therefore noise power spectrum may be pictured as the variance of a given spatial-frequency component in an ensemble of measurement of that spatial frequency.

Dainty and Shaw[14] give the NPS as

$$NPS(u,v) = \lim_{X,Y\to\infty} \frac{1}{2X\cdot 2Y} \left\langle \left| \int_{-X}^{X}\int_{-Y}^{Y} [I(x,y)-\overline{I}]e^{-2\pi i(ux+uy)}dxdy \right|^2 \right\rangle \quad \cdots\cdots (3)$$

where I is the image intensity, $\overline{I}$ is the average background intensity, and angled brackets denote ensemble average. In generally, the NPS calculation was based on a following equation[15].

$$NPS(u_n, v_k) = \lim_{N_x,N_y\to\infty} (N_x N_y \Delta x \Delta y) \left\langle \left| FT_{nk} I(x,y) - S(x,y) \right|^2 \right\rangle \quad \cdots\cdots (4)$$

$$= \lim_{N_x,N_y\to\infty} \lim_{M\to\infty} \frac{(N_x N_y \Delta x \Delta y)}{M} \sum_{m=1}^{M} \left| FT_{nk} I(x,y) - S(x,y) \right|^2 \quad \cdots\cdots (5)$$

$$= \lim_{N_x,N_y,M\to\infty} \frac{\Delta x \Delta y}{M\cdot N_x N_y} \sum_{m=1}^{M} \left\langle \left| \sum_{i=1}^{N_x}\sum_{j=1}^{N_y} (I(x_i,y_j) - S(x_i,y_j)) \exp(-2\pi i(u_n x_i + v_k y_j)) \right| \right\rangle \quad \cdots\cdots (6)$$

If one has available a fast Fourier transform (FFT), then NPS is most conveniently computed from Eq. (5). In this study, five regions of interest were selected for obtaining the NPS, the detector were uniformly irradiated at an exposure of 1.44 mR/frame. To reduce a temporal averaging effect by the image lag, we have enough time before next exposure. The calculation method used here was the noise measuring in ROI of rectangular shape (width 32 pixel & length 256 pixel). 20 frames were sequentially acquired to remove fixed pattern noise. Then first-half frames were subtracted from the later-half frames. Therefore noise power spectrum was calculated from the 10 frames. To improve precision, 10 individual power spectrum, for a total of 200 frames, were measured and averaged. Fig. 6 shows the measured NPS for digital x-ray detector using amorphous selenium. For overall spatial frequency, measurement resulting shows generally equivalent noise level.

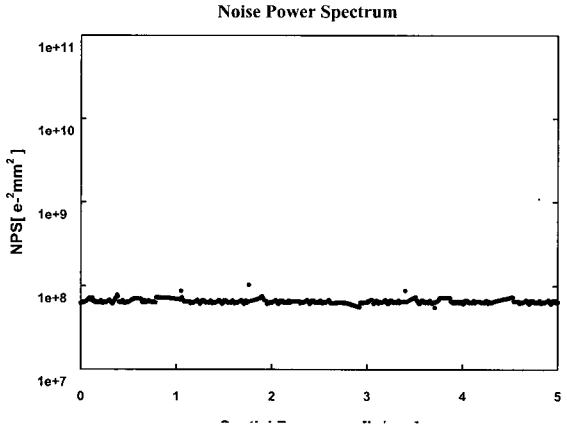

Fig. 6. Measured NPS(X-ray beam condition : 80 kVp at 1.44 mR)

5. Detective Quantum Efficiency

Detected quantum efficiency (DQE) is a parameter describing how much noise is added by an imaging system to the final image. An imaging system, such as an image intensifier, will not absorb all photons impinging on it. Some of them will be lost due to transmission. The efficiency of collecting photons is characterized by the quantum detection efficiency QDE. The detected quantum efficiency (DQE), however, is a measure of how well the imaging system utilizes the photons absorbed, and this can be thought of as how much noise is introduced by the imaging system. The DQE is thus a measure of how much noise is added by the imaging system to the quantum noise that is present in the X-ray beam incident on the imaging system.

To obtain an information about the maximum available signal-to-noise ratio as a function of frequency, We calculated frequency dependent detective quantum efficiency (DQE) from the MTF and NPS. The MTF describes the signal response of a system at a given frequency, and the NPS describes the amplitude variance at a give frequency. The calculation was based on a well-known equation[14].

$$\mathrm{NEQ}(f) = SNR^{2}{}_{output}(f) = \frac{MTF^{2}(f)}{NPS(f)} \quad \cdots\cdots (7)$$

$$DQE(f) = \frac{\mathrm{NEQ}(f)}{SNR^{2}{}_{input}} \quad \cdots\cdots (8)$$

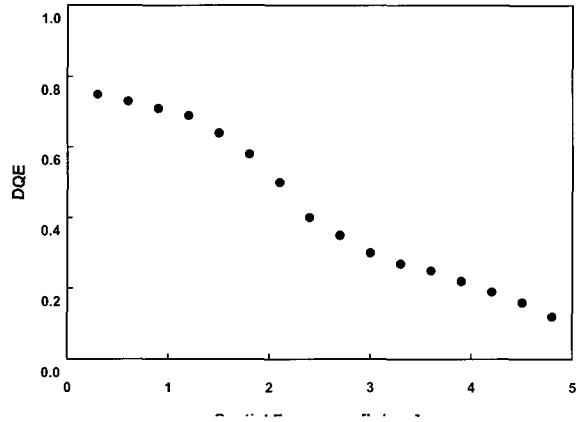

Fig. 7. Detective quantum efficiency (DQE) calculated from the MTF and NPS

$$DQE(f) = \frac{SNR^{2}{}_{output}}{SNR^{2}{}_{input}} = \frac{k^{2} \cdot MTF^{2}(f)}{\Phi_{0} \cdot NPS(f)} \quad \cdots\cdots (9)$$

Where k is the pixel x-ray response (in electrons), and Φ_0 is the mean incident x-ray fluence per unit area (in quanta/mm^2), which is determined by the measured sensitivity to the exposure and X-ray spectrum. Fig. 7 shows the calculated DQE curves for the a-Se based digital x-ray detector. The resulting DQE(0) values was about 0.75 for the detector.

6. Test images

Fig. 8 represents some digital radiographic images using by a-Se based detector. We obtained the pin-hole camera on Fig. 8(a). Finally, clinical evalution was confirmed by imaging a hand image on Fig. 8(b).

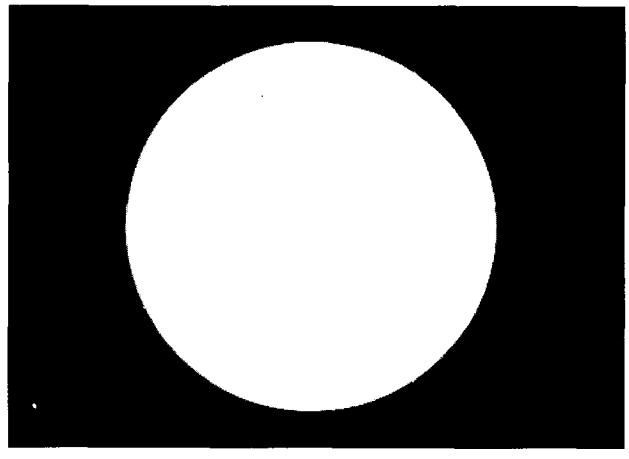

(a) 10㎛ slit camera

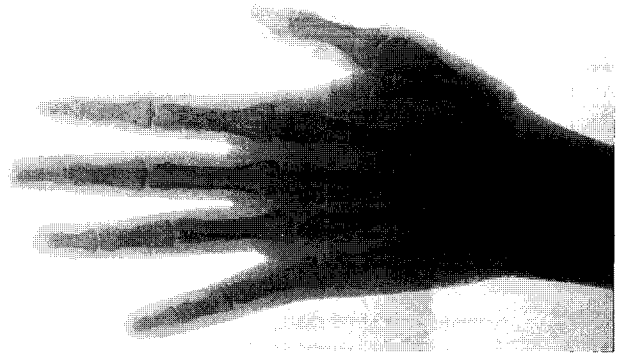

(b) hand image

Fig. 8. Image taken with the a-Se detector

IV. DISCUSSION & CONCLUSION

We have developed a direct detection flat-panel detector using a-Se, and evaluated its imaging performance with respect to sensitivity, linearity, MTF, NPS, and DQE. The measured sensitivity for the detector was 4.16×10^6 ehp/pixel · mR at the bias field of 10 V/㎛. This value is as large as that of other a-Se based digital radiography detector. And Presampled MTF showed the characteristics of unsharpness and the sampling aperture of the detector. At a cutoff frequency of 3 lp/mm, the MTF was measured as 38%. And using measured MTF and NPS, we calculated that the DQE(0) values was about 0.75 for the detector. In conclusion, for image performance evaluation, physical measurements result performed all over the general radiography range show that the a-Se based flat panel digital radiography is able to provide a superior image quality in terms of MTF(f) and DQE(f), and these results show the potential usefulness of the DR system using amorphous selenium in clinical work.

V. ACKNOWLEDGEMENTS

This work was supported by National Research Laboratory program (M1-0104-00-0149)

REFERENCE

1. Denny, L. L., Lawrence, Y. K. Cheung, Eugene F. Palecki, and Lothar S. Jeromin. "A Discussion on Resolution and Dynamic Range of Se-TFT Direct Digital Radiographic Detector." SPIE (The International Society for Optical Engineering). Medical Imaging 1996.
2. Anthony B. W.t, PhD Formerly Instructor Harvard Medical School Boston, MA and Staff Medical Physicist National Cancer Institute Bethesda, MD, "Physics of Radiology".
3. Wolbarst, A. B., Cook G., Physics of Radiology, Appleton & Lange, 1993.
4. Yaffe M. J., Rowlands J. A., X-ray detectors for digital radiography. Phys, Med, 1997 : 1~39.
5. Boreman, G. D., Modulation Transfer Functionin Optics and Electro-Optical System.
6. Ishida M, Doi K, Loo Ln, et al. Digital Image Processing : Effect On Detectability Of Simulated Low Contrast Radiographic Pattern, Radiology 1984;160:569-572.
7. Veenland, J. F. And Grashuis, J. L. Texture Analysis In Radiographs : The Influence Of Modulaiton Transfer Function And Noise On The Discriminative Ability Of Texture Features, Med. Phys. June. 1988
8. Zhao, W. And Rowlands, J. A. Digital Radiology Using Active Matrix Readout Of Amorphous Selenium : Theoretical Analysis Of Detective Quantum Efficiency, Med. Phys. Sep. 1988.
9. Shaber, Gary S., M.D., Andrew Maidment, Jeffrey Bell, Lothar Jeromin, Denny Lee, and Gregory Powell. "Full Field Digital Projection Radiography System : Principles and Image Evaluation." Computer Assisted Radiology and Surgery (CAR '97). by H. U. Lemke, et. al., editors. (Amsterdam : Elsevier, 1997), pp. 39-45.
10. Denny, L. L., Lawrence Y. K. Cheung, Lothar S. Jeromin, and Eugene F. Palecki. "Imaging Performance of a Direct Digital Radiographic Detector Using Selenium and a Thin-Film-Transistor Array." Computer Assisted Radiology. by H. U. Lemke et al., editors., pp.41-46.
11. J Beutel J., Kundel, H. L., Handbook of Medical Imaging. SPIE.
12. Fujita, H., Tsai, D. Y., Takumi Itoh Kunio Doi, A Simple Method for Determining the Modulation Transfer function in Digital Radiography, IEEE Transactions on Medical Imaging, Vol. 11, NO. 1, Mar 1992.
13. Fujita, H., et al. Investigation of basic imaging properties in digital radiography ; MTFs of II TV digital imaging systems. Med. Phys. 1985, Nov./Dec.

14. Dainty, J. C. and Shibata, N., Image Science (Academic Press, New York, 1974).

15. James T. Dobbins Ⅲ, Handbook of Medical Imaging, vol 1, chap 3, SPIE press.

• 국문요약

평판 디지털 X-ray 검출기의 개발과 성능 평가에 관한 연구

박지군 · 최장용 · 강상식 · 이동길 · 석대우 · 남상희*

*인제대학교 의용공학과 · 인제대학교 의료 영상 연구소**

의료영상 분야에서의 디지털화가 시도되면서부터 평판형 디지털 영상검출기가 일반촬영 및 투시영상을 비롯한 다양한 영상 획득 장치에의 적용을 위해 꾸준히 연구, 개발되어져 왔다. 본 연구는 비정질 셀레늄을 이용한 디지털 방사선 검출기를 통해 획득된 영상의 평가를 통해 순수 국내 기술로 개발중인 디지털 방사선 검출기의 임상 사용여부를 확인하고, 영상평가의 주요인자인 modulation transfer function (MTF), noise power spectrum (NPS), and detective quantum efficiency (DQE) 이용하여 정량적인 값을 도출함으로써 의료영상평가에 필요한 측정 방법 및 그 기초 자료의 제공을 그 목적으로 한다. 비정질 셀레늄을 이용한 디지털 방사선 검출기는 pixel pitch가 139 ㎛이며, 전체 active area은 14×8.5 $inch^2$, 전체 pixel의 수는 3.9백만개이다. 디지털 X-선 검출기에서 광도전체로서 비정질 셀레늄은 TFT 평판 패널 위에 진공 증착된다. 비정질 셀레늄의 두께는 500 ㎛이다. 디지털 방사선 검출기의 성능을 평가하기 위해 민감도, 선형성, MTF, NPS, 그리고 DQE가 측정되었다. 선형성 평가에서는 뛰어난 선형성[(r^2) = 0.9693]을 보였다. 측정된 민감도는 인가전압 10 V/㎛에서 4.16×10^6 ehp/pixel · mR이며, MTF는 2.5 lp/mm에서 52%이다. 그리고 DQE는 1.5 lp/mm에서 75%이다.

본 연구를 통해 영상평가 측정 기술의 기본적 토대를 마련하고, 측정된 값은 국내 기술로 개발중인 비정질 셀레늄을 이용한 직접방식의 디지털 방사선 검출기의 임상적 사용가치가 충분함을 뒷받침할 수 있는 기초 자료로서 제공될 수 있을 것으로 판단된다.

key wards : 평판형 디지털 방사선 검출기, 셀레늄, TFT, 민감도, 선형성, MTF, NPS, DQE